Summary of the stratigraphy of both foot- and hanging-wall exposures of the Cliff fault, southern embayment of the Albuquerque Basin, Socorro County, New Mexico

David W. Love, Eda Celep, David J. McCraw, and Daniel J. Koning

2022, pp. 253-263. https://doi.org/10.56577/FFC-72.253

in:

Socorro Region III, Koning, Daniel J.; Hobbs, Kevin J.; Phillips, Fred M.; Nelson, W. John; Cather, Steven M.; Jakle, Anne C.; Van Der Werff, Brittney, New Mexico Geological Society 72nd Annual Fall Field Conference Guidebook, 426 p. https://doi.org/10.56577/FFC-72

This page is intentionally left blank to maintain order of facing pages.

New Mexico Geological Society Guidebook, 72nd Fall Field Conference, 2022, p. 253–263.

SUMMARY OF THE STRATIGRAPHY OF BOTH FOOT- AND HANGING-WALL EXPOSURES OF THE CLIFF FAULT, SOUTHERN EMBAYMENT OF THE ALBUQUERQUE BASIN, SOCORRO COUNTY, NM

DAVID W. LOVE[1], EDA CELEP[2], DAVID J. MCCRAW[1], AND DANIEL J. KONING[1]

[1]New Mexico Bureau of Geology and Mineral Resources, New Mexico Institute of Mining and Technology, 801 Leroy Place, Socorro, NM 87801; david.love@nmt.edu
[2]1501 Elm Street, Fort Collins, CO 80521

Abstract—The Cliff fault, an 8.2 km long, north-striking, down-to-the-west normal fault offsetting basin fill of the southwestern Albuquerque Basin of the Rio Grande rift, exposes lithofacies primarily derived from the Rios Salado and Puerco that are about 120 m thick in the footwall and at least 65 m in the hanging wall. Both the footwall and hanging wall form elevated ridges adjacent to the fault, with erosional D-shaped badland "bowls" that drain eastward across the fault into the Rio Grande Valley. The fault trace has been differentiated into seven quasi-linear geographic extents based upon directional changes in the fault trace, erosional elevation differences between the footwall and hanging wall, types of contacts of the hanging wall with the fault, amounts of erosion in headwater bowls and in a southern tributary, and capping Rio Salado terrace gravels.

The footwall lithostratigraphy grades upward from basal, southeast-trending Rio Puerco pebbly sand channels and overbank silty fines into a mixed source architecture containing narrow, pebbly sand channels with Rio Salado–type clasts. At the north end, gravel and pebbly sand beds contain the 3.5 Ma Grants obsidian. The upper footwall cliffs are dominated by Rio Salado well-cemented conglomerates and sandstone ledges, but also have fine-grained alluvial facies, semiarid pedogenic carbonate soil horizons, and eolian dunes. Exposed in the erosional bowls in the hanging wall are five distinct, fault-derived or modified lithofacies, truncated by four post-fault channel deposits, including two Rio Salado stream terraces. An estimate of erosional stripping of as much as 27 m of the footwall, down to a 7° slope to the fault, was calculated using scarp-related debris on the hanging wall (15 m thick over an area with a 2° slope), which yields roughly 3075 m^3/m along the fault.

These findings correct previous paleogeographic interpretations, because the ancestral Rio Salado flowed northeast into the Albuquerque Basin during Pliocene time before turning southeast to join the ancestral Rio Grande near the Joyita Hills and sometimes joining the Rio Puerco. This results in a southwestern basin floor facies (floodplain and fluvial/alluvial sediment interfingering with distalmost fan lobes) to the southeast. Movement of the Cliff fault episodically followed; displacement phases are recorded in the five distinct hanging-wall lithofacies. After cessation of fault activity sometime in the early Middle Pleistocene, the Rio Salado drainage deposited terrace gravel, and later a northern tributary deposited alluvium that buried the Cliff fault near its southern extent. Subsequent Rio Grande Valley erosion has removed most evidence of episodes of terrace formation inset against the footwall, as well as most of the footwall sediments.

INTRODUCTION

Basin fill of the southern Albuquerque Basin of the Rio Grande rift west of the Rio Grande has been mapped but not studied in detail (Denny, 1940; Machette, 1978a, b; Love and Young, 1983; Connell et al., 2001; McCraw et al., 2006; Connell and McCraw, 2007). Albuquerque Basin fill farther north has received more study (e.g., Bryan, 1938; Lambert 1968; Kelley, 1977; Hawley, 1978; Connell, 2008; Connell et al., 2013). Machette (1978a) named the Sierra Ladrones Formation for Plio-Pleistocene deposits in the southern Albuquerque Basin related to the arrival of the ancestral Rio Grande, reflected in both axial-fluvial pebbly sands and coarser, poorly sorted piedmont alluvium. Machette (1978a) mapped all exposures along the Cliff fault (Fig. 1) as Sierra Ladrones Formation piedmont alluvium and interpreted them as an alluvial apron derived from the Joyita Hills to the southeast. Connell (2008; Connell et al., 2013) brought his redefined Ceja Formation south from the Albuquerque area to be applied to all upper basin-fill deposits derived from the west side of the Albuquerque Basin and restricted the Sierra Ladrones Formation to the fluvial facies of the ancestral Rio Grande and to piedmont facies from the east side of the basin. Connell and McCraw (2007) mapped what had been Sierra Ladrones Formation at the northwestern end of the Cliff fault as Ceja Formation. Connell (2008) described the Ceja Formation west of Albuquerque primarily as having sandy and gravelly channels with fine-grained overbank deposits, eolian sand dunes and sand sheets, and pedogenic carbonate soils. Many of these strata are related to the paleo-distributary system of the Rio Puerco. Similarly, Davis et al. (1993) mapped a small area of Sierra Ladrones Formation (now Ceja Formation) about 22 km north of the Cliff fault to describe and analyze the permeability of four facies or architectural elements of basin fill. They delineated gravel channels and filled, arroyo-like sandy channels with sandy overbank deposits extending above and beyond the incised arroyo margins. These facies are a distal part of the ancestral Rio Puerco–Rio San Jose depositional system. Davis et al. (1993) traced three types of soils related to the parent materials of clay, sand, and gravel. They did not separate the thin eolian deposits as part of the system.

Paleogeographic maps of the former paths of the ancestral Rio Grande and its tributaries in the Albuquerque Basin were produced first by Bryan (1938) and his students (Denny, 1940;

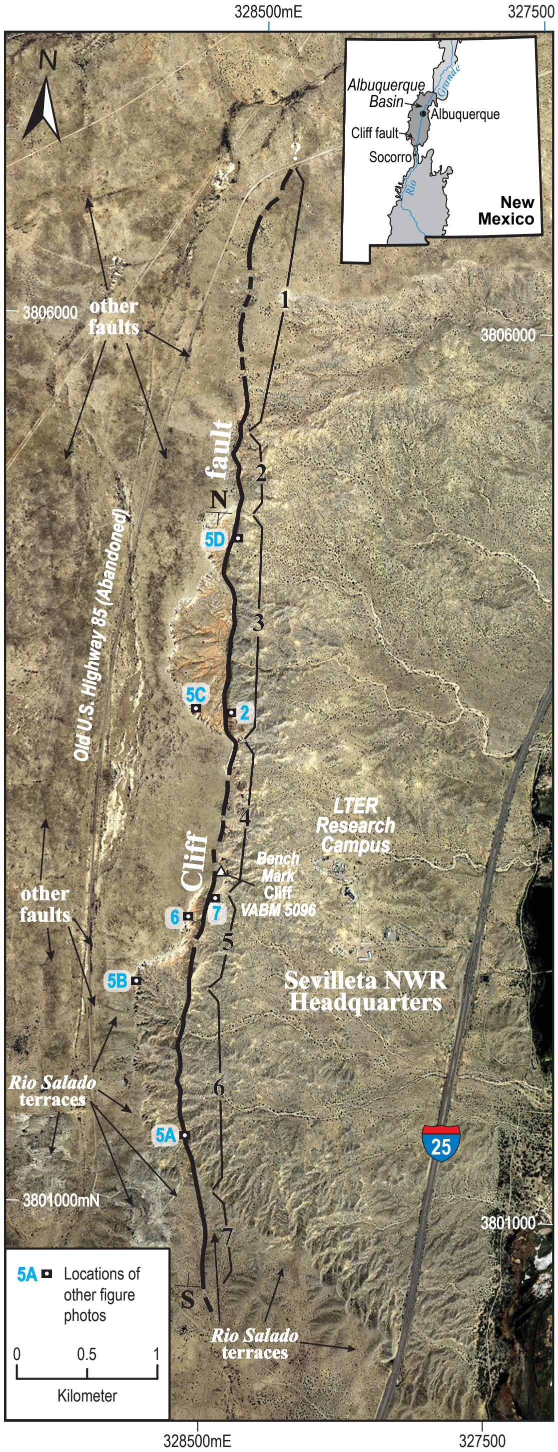

FIGURE 1. Location of the Cliff fault in the southern Albuquerque Basin of the Rio Grande rift in New Mexico. Divisional extents of the trace of the Cliff fault are, from north to south: (1) footwall higher than deposits of hanging wall; (2) hanging wall higher than footwall; (3) hanging wall higher than footwall, but both are eroded with development of D-shaped erosional headwater bowls draining east; (4) footwall higher than hanging wall, and hanging-wall deposits in contact with the footwall across trace of fault; (5) eroded footwall higher than hanging wall, with small erosional bowls cutting across fault and hanging wall; (6) footwall lower than hanging wall, with larger erosional bowls; western drainage divide capped by terraces of the ancestral Rio Salado; and (7) fault trace enhanced by erosion along a short valley dissecting terraces with no apparent offset between footwall and hanging wall. Fault trace not apparent to south across lower Rio Salado terrace. Camera symbols locate where photos of Figures 3–8 were taken. Photo base modified from Google Earth.

Wright, 1946). Bryan and Denny thought that the ancestral Rio Grande veered southeast from the Bernardo area and exited the Albuquerque Basin toward the northern Jornada Basin. Modifications of the mapped river's course have been relatively consistent (e.g., Lozinsky et al., 1991; Davis et al., 1993; Connell et al., 2001, 2013). The maps show the fluvial Rio Grande deposits as a narrow ribbon down the east-central part of the basin. All the maps show the contributions of the generalized Rio Puerco drainage to the fill of the western half of the basin, but none of the maps has recognized the large contribution of the ancestral Rio Salado to the southern Albuquerque Basin, which could potentially influence the course of the Rio Grande to the southeast.

The isostatic residual gravity map of the southern Albuquerque Basin of the Rio Grande rift (Fig. 2; Gillespie et al., 2000; Grauch and Connell, 2013; Celep, 2017) shows that the deepest part of the southern basin is northeast of Bernardo, with a southern extension of the basin as a north-plunging syncline between two north-south-trending Quaternary faults with surface expression. West of the syncline is the down-to-the-east Loma Blanca fault, and above, or slightly to the east, of the interpreted gravity syncline is the down-to-the-west Cliff fault (Fig. 2). In the Los Lunas area farther north in the Albuquerque Basin, the active rift faults tend to have stepped from the rift margins toward the center of the basin, suggesting a basinward transfer of strain (Olig et al., 2011, and references therein). In the southern Albuquerque Basin, the distribution of strain is less clear (Grauch and Connell, 2013). The Cliff and Loma Blanca faults appear to be toward the basin center, but they are among several recently active Quaternary faults. Near the western basin edge lies the normal, down-to-the-east Loma Pelada fault (Machette and McGimsey, 1983). To the east of our study (Fig. 2) is the down-to-the-west Contreras Cemetery fault (McCraw et al., 2006), the Maes-Abo fault zone, the down-to-the-east Military Road fault (Rinehart et al., 2014), and the least-active Los Pinos fault. Shorter faults with less surface offsets exist between these more active faults, but remain unstudied.

Erosion along the west side of the Rio Grande Valley, east of and along the Cliff fault, exposes about 120 m of basin fill of the footwall and at least 65 m of hanging-wall strata. The damage zone along the Cliff fault is commonly exposed and may be traced nearly 8 km. This summary of these exposures is based on detailed study of the northern exposures of deposits on both sides of the Cliff fault by Celep (2017) and by ongoing unpublished investigations by Love and McCraw.

DESCRIPTION OF THE FAULT TRACE

The Cliff fault is a north-south, down-to-the-west normal fault shown on maps by Denny (1940), Machette (1978a, b), Machette and McGimsey (1983), Grauch and Connell (2013), USGS Quaternary fault and fold database (Cliff fault No. 2111, accessed 1/21/22), and Celep (2017; Fig. 1). Its exposed trace is approximately 8.2 km long. Both stream valleys of modern Rios Puerco and Salado truncate and/or bury the extent of the fault to the north and south, respectively. Machette and McGimsey (1983) and Connell and McCraw (2007) interpreted

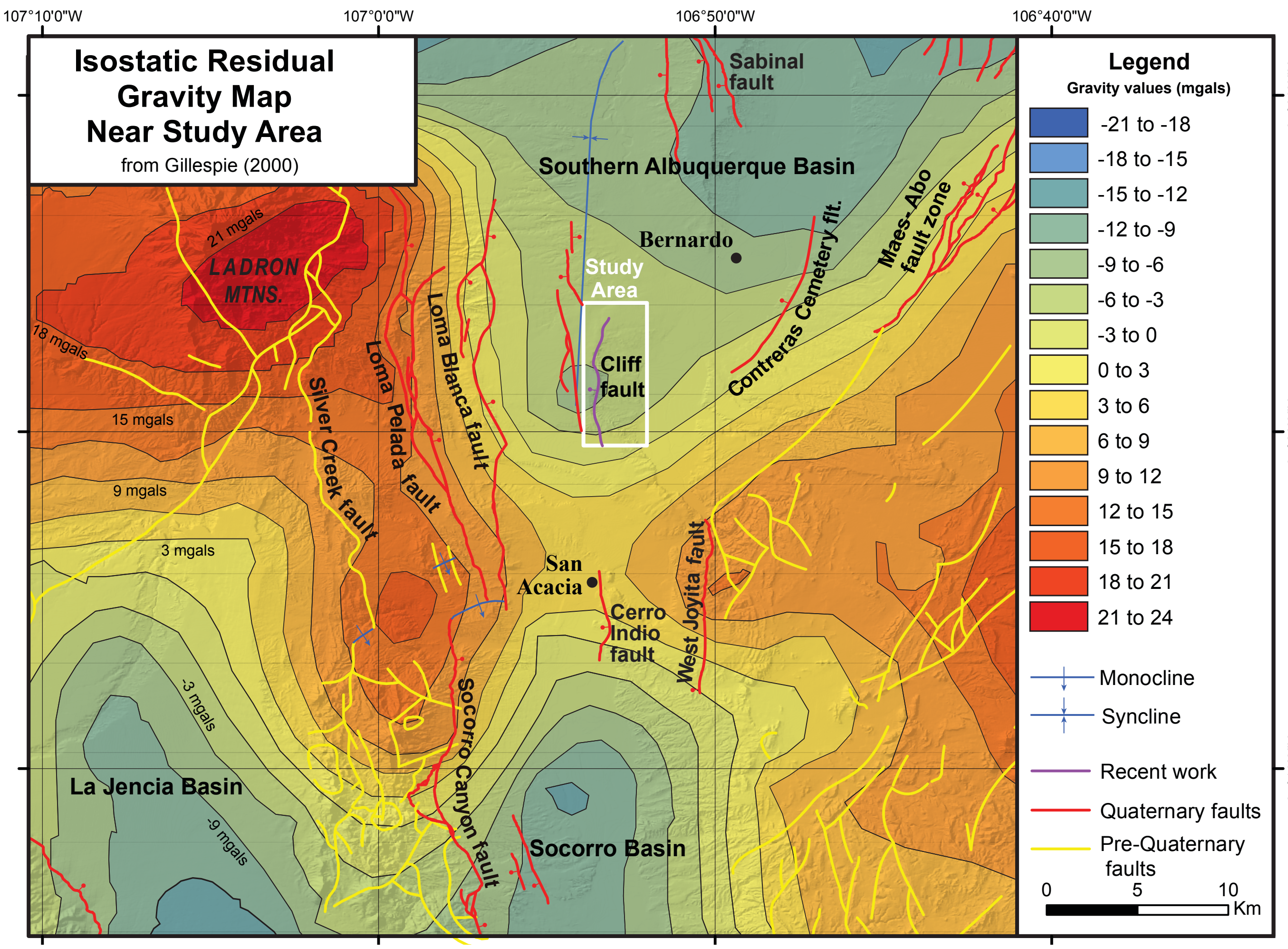

FIGURE 2. Location of the Cliff fault in the southern Albuquerque Basin in relation to other Quaternary faults and the isostatic residual gravity map (modified from Gillespie et al., 2000, and Celep, 2017).

that, at the northern end, the fault turns northwest and cuts younger piedmont deposits, but we trace the footwall of the main Cliff fault north to the north-northeast (Fig. 1) so that the northwest-trending younger fault is a different structure. Some previous workers have interpreted the southernmost Cliff fault to connect to the south-southeast to the fault on the west side of Cerro Indio (Indian Hill; Machette, 1978a; Machette and McGimsey, 1983; Sion et al., 2016; Celep, 2017). But hanging-wall offset along the Cliff fault decreases along southern exposures, suggesting that the Cliff fault dies out and does not directly link with the fault near Cerro Indio. Therefore, the structure to the south may have a relay ramp between the two faults. West of the Cliff fault are up to four apparently younger fault traces seen on aerial photographs and Google Earth (Fig. 1). These unstudied faults appear to cut younger alluvium in terraces and along valley floors.

The present maximum elevation of the footwall is marked by the Bench Mark VABM Cliff at 5095 ft (1553 m). Erosion of the footwall has resulted in notable lowering of the paleosurface between the Cliff fault and the Rio Grande floodplain, which now lies 120 m below the benchmark. The footwall and hanging wall form an elevated ridge or two sub-parallel ridges adjacent to the fault, with erosional D-shaped badland “bowls” developed across the fault that drain into the valley from the looser sediments of the down-faulted hanging wall.

We divide the trace of the Cliff fault into seven quasi-linear geographic divisions or extents (Fig. 1). These are not fault behavioral segments, because there is no evidence that parts of this short fault moved separately or more frequently than other parts. The divisions are designated based upon directional changes in the fault trace and erosional patterns of the footwall, hanging wall, stream terraces, and tributary valley alluvium. From north to south, the divisions are (1) from the northern limit of the elevated footwall in the Rio Puerco Valley south along the western eroded edge of the footwall; (2) southward the fault trends slightly southeast, and the preserved hanging wall becomes higher than the eroded footwall; (3) farther south, erosional headwater bowls drain eastward, crossing the footwall, fault, and hanging wall, the drainage divide shifts to the west, and the hanging wall is higher than the eroded footwall; (4) the hanging-wall alluvium meets the erosional fault-line scarp and the eroded footwall is higher than the hanging wall; (5) two eastward-draining, small erosional bowls developed in the hanging wall cut through the higher, eroded footwall; (6) an area of eastward-draining larger erosional bowls where the hanging wall is higher than the footwall and the western divide of the bowls is capped by high terraces of the Rio Salado; and (7) the southernmost extent of the fault trace where both the footwall and hanging wall are capped by Rio Salado terrace gravel at similar elevations. The fault trace forms an eroded scarp of partially cemented gravel of the footwall in an erosional, south-draining tributary valley of the modern Rio Salado, and alluvium at the head of the valley is deposited across the fault trace. Collectively, the fault trace divisions have a northward strike, varying from N38°W to N28°E over distances of 10s to 100s of meters. Because there are several erosional bowls along the fault, we refer to these bowls as part of their geographical extents, e.g., Division 3 north and south, Division 5 north and south, and Division 6 north and south (Fig. 1).

DESCRIPTION OF THE FAULT DAMAGE ZONE

The damage zone, exposed in meters-long swaths along the Cliff fault, varies both vertically and horizontally. The fault dips westward from 70° to vertical, mostly between 80° and 90°. In general, sedimentary units in the footwall are only locally tilted toward the fault within a few meters of the fault. Footwall exposures of both conglomeratic and fine-grained units show that the units are nearly planar over several kilometers parallel to and eastward, away from the fault. On the footwall side of the damage zone, particularly adjacent to conglomeratic beds, the pebbly sand caught in the damage zone is cemented parallel to the fault zone, with 0.2–3.0 m of phreatic calcium carbonate and locally with dark stains of iron and manganese-oxides and hydroxides. The cemented footwall side of the damage zone crops out along the fault all the way to the surface. The central interior of the damage zone consists of sheared, commonly reddish-brown or brownish-gray clay. The width of this zone ranges from a few centimeters to several meters (Fig. 3).

FIGURE 3. View north along the damage zone of the Cliff fault, illustrating massive cementation along the edge of the footwall and upturned, fine-grained, smeared beds of the hanging wall.

The lower units on the hanging-wall side of the damage zone commonly consist of sand, silt, and clay that are warped up several meters along the fault and/or have stepped minor offsets down to the west in tilted beds west of the fault. The lower exposures of hanging-wall sediments commonly have local cemented nodules, but are not pervasively cemented like the footwall except along the southernmost exposed Division 6, which exhibits northeast-tilted (toward the fault), cemented, conglomeratic and fine-grained units similar to those in the footwall. The predominantly sandy hanging-wall units in mid-level exposures of the hanging wall meet the fault nearly horizontally, whereas the upper-level, predominantly sandy units—even though they have been dropped down—appear to have been deposited on a slope tilted to the west away from the fault. Their contact with the fault commonly has just a thin (<30 cm) damage zone.

STRATIGRAPHY OF AND FACIES OF THE FOOTWALL

About 120 m of footwall strata are exposed between the floodplain of the Rio Grande and the top of the footwall at the Cliff benchmark. The upper part of this section was described by Celep (2017). The upper cliffs are somewhat protected from erosion by well-cemented capping conglomerates. Below this cap lie conglomerates interbedded with tan and pale brown sands and sandstones, dark reddish-brown sandy clays, and pedogenic carbonate soil horizons collectively representing basin-floor and local alluvial-fan facies (Fig. 4). There are minor eolian sand dunes with slip faces more than 3 m high preserved locally. Poorly sorted, slightly muddy sand with scattered pebbles are inferred to be hyper-concentrated flow deposits. The coarse conglomerates have southeastern to southerly transport directions, whereas the loose gravels and sandstones have a variety of flow directions from northeast to south. The coarse Rio Salado conglomerates at the top of the section at the northern edge of exposures contain large cobbles and boulders of 3.24 Ma Riley travertine (Lueth et al., 2016).

Below the cliffy exposures are less-cemented, more-erodible strata comprised of Rio Puerco and Rio Salado deposits. The lower parts of the section appear to be dominated by southeast-transported Rio Puerco pebbly sand channels, tan overbank sandy silts, and thin brown or reddish-brown clay beds (Connell et al., 2001). The middle part of the footwall section has similar basin-floor sands, silts, and clays with Rio Puerco–like channels, but also has some narrow, trough cross-bedded, pebbly sand channels with Rio Salado–type clasts (Celep, 2017). At the north end of exposures, broad gravel beds or pebbly sand beds have clasts derived from both the Rio Salado and Rio Puerco with transport to the southeast. Some of these channels contain 3.5 Ma obsidian from the Grants area (F. Goff and S. Shackley, pers. commun., 2022; cf. Love and Young, 1983; Young and Love, 2016). It is probable that the Blancan fossil horse tooth and fragmentary stegomastodon bones (reported by Denny, 1940; Morgan et al., 2009) came from this stratigraphic interval and are also about 3 Ma.

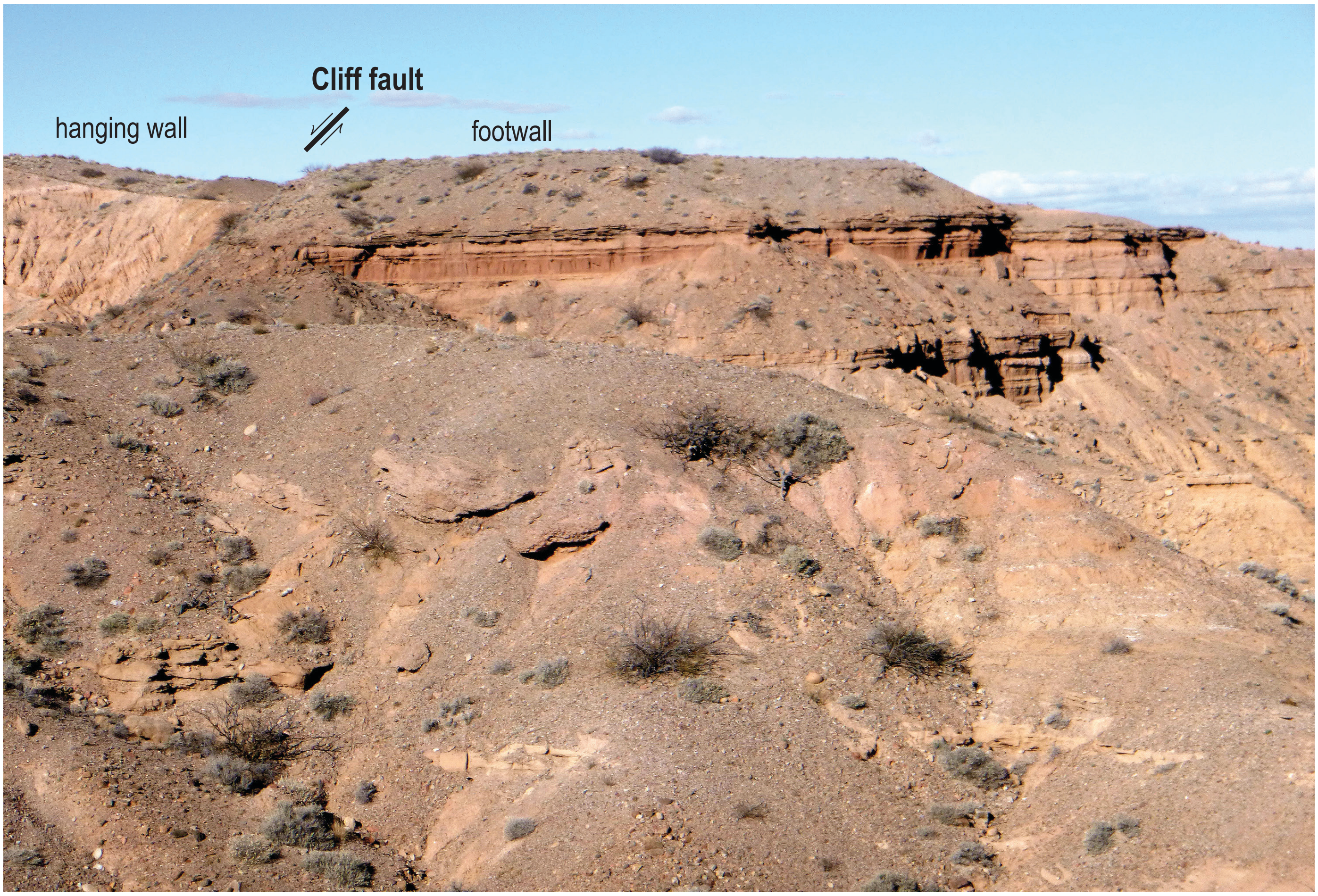

FIGURE 4. Footwall of the Cliff fault illustrating cliffs held up by coarse conglomerates with finer-grained facies between, representing ponded red-brown clay, distal alluvium as fans, eolian sand, and other basin-floor sediments. Below the conglomeratic cliff interval are finer-grained overbank/basin-floor beds and smaller channels from the Rio Salado and Rio Puerco, both exhibiting southeast transport. Upper coarse conglomerates containing large clasts of the ancestral Rio Salado show south, southeast, and east transport directions; these are better cemented than the underlying beds. The Cliff fault and elevated deposits of the hanging wall are exposed in the upper left corner of the photo at the junction of fault trace Divisions 2 and 3.

STRATIGRAPHY OF THE HANGING WALL AND POST-FAULT DEPOSITS

Detailed stratigraphy of the hanging wall of the Cliff fault is extensively exposed in erosional bowls parallel to and west of the north trend of the Cliff fault. A south-to-north profile along the base of hanging-wall exposures and west-looking view of hanging-wall stratigraphy shows about 65 m of exposures (Fig. 5). We depict five simplified units and four post-hanging-wall deposits. The oldest deposits of the hanging wall (unit 1, southern bowl of Division 6) consist of (i) pale brown beds of fine sand, silt, and brown or reddish-brown clays overlain by (ii) 2–3 m of well-cemented, pebbly sandstone and conglomerate that dips up to 14°NE toward the Cliff fault (Fig. 6A). These are overlain by (iii) less-consolidated, pale brown and orangish sands, silts, and clays, stage II pedogenic calcium-carbonate horizons, and a few multistory conglomerate channels having pebble imbrications indicating south, southeast, and slightly southwest transport. The upper part of this group of beds dips to the northeast toward the cliff fault at 4–6°. The top of unit 1 is capped by a couplet of white-gray, carbonate-cemented sandstone or pebbly sand overlain by a reddish-brown bed that varies from pebbly gravel in southwestern exposures to clay beds up to 3 m thick, with local pebble-sized gravel in the middle, close to the Cliff fault. The white to very pale greenish-gray bed is commonly less than 60 cm thick but can be more than a meter thick. It has a sharp lower contact with underlying sand, and this bed is interpreted as having been influenced by shallow groundwater under reducing conditions (hence reduced iron hydroxides). This lowest unit (1) is 18 m thick and is interpreted to exhibit the same type of deposits as those exposed in the footwall, offset and tilted northeastward at the south end of the Cliff fault. As such, we interpret unit 1 as basin-floor deposits with south-flowing channels of the Rio Salado and as being a preserved section of the footwall tilted northeastward toward the Cliff fault. We interpret the wedge-shaped, reddish-brown clay at the top as perhaps the first, and lowest, ponding of fine-grained sediments against the fault scarp.

The overlying pebbly sand deposits (divided into two units for mapping purposes by Celep, 2017) are lumped into unit 2 in Figure 5 (primarily in the northern bowl of Division 6). This unit appears to be conformable, but with a scoured base cut into the reddish-brown clay of unit 1 also dipping about

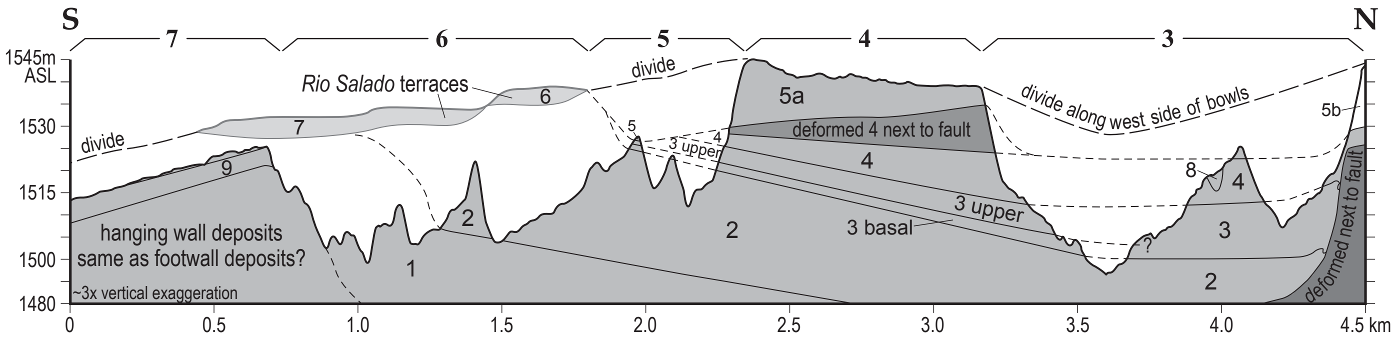

FIGURE 5. South-north topographic profiles of the base of erosional bowls, western drainage divides, Divisions 3–7, and cross section of hanging wall units parallel to the Cliff fault, illustrating five composite depositional units of the hanging wall and four post-fault depositional episodes preserved in cross-cutting deposits. Profile modified from Google Earth with three times vertical exaggeration.

5°NE toward the Cliff fault. Uppermost strata of unit 2 dip about 1.6°N (Figs. 5, 6B). The bulk of the unit is pebbly sand in broad, shallow channels (locally cemented into sandstone ledges) and locally incised channels with pebble imbrications to the south or southeast. Adjacent to the fault are one or more reddish-brown clayey units <1.3 m thick that wedge out to the west-southwest. Unit 2 also has carbonate paleosols developed in some sandy strata. The top of this unit has a paleosol with a pale reddish-brown Bt horizon above a stage II pedogenic carbonate horizon. This composite unit is about 25 m thick. Unit 2 represents a stack of south-flowing Rio Salado pebbly sand channels paralleling the Cliff fault. Minor wedge-shaped, red-brown clay facies next to the fault may represent local ponding events related to offsets along the Cliff fault. No fault scarp–related debris was noted in this unit.

At the northern end of the northern bowl of Division 6, the conformable base of unit 3 consists of a wedge-shaped, reddish-brown, silty-clay bed up to a meter thick (Fig. 6B, C). Overlying the basal clay are beds of tan pebbly sand, tan fine sand, silt, brown and reddish-brown silty clay, and another pedogenic carbonate soil. Unit 3 exposures in the erosional bowls to the north in Division 5 consist of 6–12 m of four 1–4 m beds of reddish-brown clay, tan sand and silt, with a pedogenic carbonate soil horizon, and is capped by a thick pedogenic soil with a stage II+ carbonate horizon. In the two bowls of Division 3, Celep (2017) interpreted one of the beds lumped into this unit to have been shed westward from the footwall. The largest and deepest erosional bowl (Division 3, south bowl) cut into the hanging wall has more and thicker units than those exposed to the south (Celep, 2017). The lower beds dip to the northeast toward the Cliff fault and are folded upward and smeared out against the fault. They locally show at least two minor angular unconformities near the fault and appear to be folded into a very broad, shallow syncline plunging to the east. The upper units and capping soil are also dragged upward close to the fault, but are nearly horizontal to the west-southwest. The wedge-shaped, clayey units are interpreted to be playa-like deposits ponded against the scarp of the Cliff fault and perhaps dammed locally along the scarp by small alluvial fans distributed to the east from a larger alluvial source to the west.

Unit 4 is 11 m thick in the northern bowls (Fig. 6C), but it thins to the south and is truncated by erosional scours at the base of the overlying unit 5a. The basal pebbly sand beds of the unit rest on the underlying soil of unit 3. The lowest beds are orangish-reddish-brown sand with calcium carbonate nodules, whereas the pebbly sand above is mostly pale gray to tan and lacks nodules. Both of these units have pebble imbrications indicating transport to the north, northeast, or east, although one of the pebble beds coarsens to the northeast toward the fault (Celep, 2017). Except for the latter, these pebbly beds are interpreted to represent alluvial fan deposition with northeast-directed paleoflow. Above the pebbly sand are beds of tan silt and clay, tan sand, and the uppermost reddish-brown clay, marking a return to ponded clay deposition on the hanging wall. The fine-grained upper beds crop out in the northern bowl of Division 5 to the south, but are thinner. Farther south they are truncated by erosion at the base of unit 5a. Above the highest clay bed is one stage III pedogenic soil in the central bowl, whereas to the north there are two pedogenic stage II soils stacked above the uppermost clay. The degree of soil development on top of unit 4 suggests 10 to several 10s of ky of stability occurred (Gile et al., 1981), presumably concomitant with no notable movement along the Cliff fault.

Units 5a and 5b are the highest deposits of the hanging wall related to normal movements of the Cliff fault. Unit 5a consists of pebbly to bouldery sand deposited against the Cliff fault (Fig. 7). At least four "cycles" of coarse–sandy gravel beds are overlain by pebbly sands lacking bedding or other sedimentary structures. The pebbly sands may be a combination of pebbles and sand from the footwall and eolian sand recycled from surficial deposits of the hanging wall farther to the west. The coarse gravels die out to the west-southwest, where there are poorly developed pedogenic carbonate horizons in the section. Paleoflow of the shallow gravel channels appears to be to the west and southwest. The lower gravel beds are nearly horizontal, except near the fault. The upper beds slope away from the footwall but are cut by the fault. The stage III carbonate horizon at or near the top of exposures does not appear to be offset by the fault, but does not cross the fault onto the footwall, because the footwall is a coarse conglomeratic sandstone without a pedogenic overprint. Local late Holocene shallow channels, slopewash, and eolian sheet sands cross the trace of the fault scarp and are not offset.

Considering the lack of a fault scarp (only a low fault-line

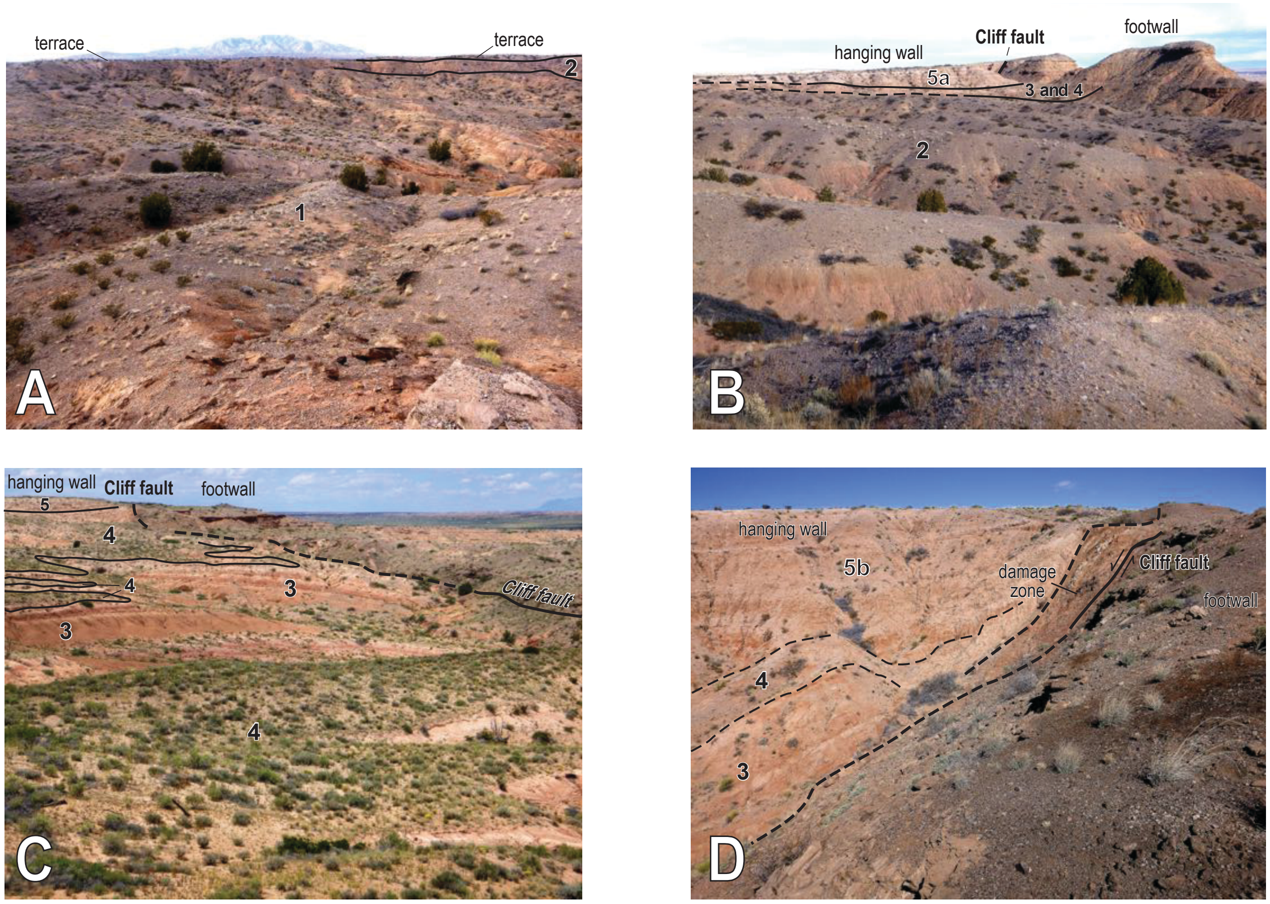

FIGURE 6. Stratigraphic units exposed in erosional bowls along the hanging walls of the Cliff fault. (A) View to northwest of large erosional bowl of Division 6 from the south end; this bowl exposes northeast-dipping, footwall-like conglomerates, sandstones, and fine-grained beds of unit 1. The western drainage divide is capped by the two terraces of the Rio Salado. Ladron Mountains are in the distance to the northwest. (B) View northeast toward Division 5 of the Cliff fault showing upper part of pebbly sand and gravel of hanging-wall unit 2 capped by a pedogenic calcium carbonate horizon (in distance), overlain by reddish-brown, wedge-shaped playa clay of unit 3, thin unit 4, and pale upper hanging-wall deposits of unit 5a. Eroded footwall to northeast is higher than the hanging wall. (C) View northeast toward the footwall of the Cliff fault (Division 3), across large erosional bowl of hanging wall. Note rollover of hanging-wall beds toward the Cliff fault. Reddish-brown clay beds wedge out to the west. (D) View north along the Cliff fault showing footwall, fault damage zone, and deformed hanging wall strata of unit 5b at the north end of exposures. Unit 5b is approximately 13 m thick. Shallow pebble gravel channels in the upper part of the section show south and southwestward transport directions. In foreground are clasts of footwall conglomerate with iron and manganese oxide coatings.

eroded scarp) along Division 4, the present accumulation of coarse gravel by local weathering, and erosion of conglomerate of the footwall, we suggest that the sand and gravel “cycles” in unit 5a may be episodic transport by large flow events across the fault prior to offsets, rather than as debris related to renewed uplift along the scarp. This summary cannot go into the details of deposition of the 15 m of unit 5a, but the cycles probably record several episodes of offset along the Cliff fault. The thickness of deposits here would compare to the 19 m of accumulated fault-scarp sediments and soils of the County Dump fault near Albuquerque (McCalpin et al., 2006), 5 m studied by Personius and Mahan (2003), and 15 m by Olig et al. (2011). These studies near Albuquerque indicate the large contributions of eolian sand to scarp-adjacent hanging walls in the northern Albuquerque Basin.

Farther north, in the northern bowl of Division 3, unit 5b is similar to 5a, consisting of mostly structureless pebbly and cobbly sand beds and some poorly developed pedogenic carbonate horizons, but local channels show transport to the south or south-southwest, subparallel to the fault rather than to the west or southwest, perpendicular to the footwall and scarp (Fig. 6D). The pebble/sand ratio increases to the northeast toward the fault, and the clasts increase in size next to the footwall. These observations support an inference that the sediment was locally eroded off of the adjacent fault scarp and then transported southward parallel to the fault by an ephemeral drainage. The top of the hanging wall has a stage III pedogenic carbonate soil horizon with the overlying Bt(?) horizon mostly stripped away. Machette et al. (1997) described the stage III soil farther west on the divide of the south bowl of Division 3. The lack of deposits on top of the stage III calcic soil implies surficial stability for at least a few 10s of ky and an end of notable offset along the fault.

As shown on Figure 5 at the southern part of Division 5 (northern edge of the northern bowl of Division 6), between outcrops along lowest exposures of the hanging wall and the drainage divide on hanging-wall units farther west, the soil at the top of unit 2, the thin edges of units 3 and 4, and all of unit 5a pinch out and are truncated by terrace gravel of unit 6, resting on the pebbly sands of unit 2.

FIGURE 7. View north-northeast of central erosional bowl south of the highest part of the footwall (Division 5), with deformed reddish-brown playa beds warped up against the fault and pale, cyclic sand and gravel beds of unit 5a at the top of exposures against the fault. Unit 5a is approximately 15 m thick.

Units 6 and 7 consist of coarse cobble-boulder gravel unconformably deposited across eroded exposures of units 1 and 2 (Fig. 5). The terrace tread to the north (unit 6) is about 5 m higher than the tread to the south (unit 7). Both treads slope down to the southeast with an apparent gradient of only 0.26 m/km. The higher terrace is about 85 m above the Rio Salado channel and about 96 m above the Rio Grande. The boulders and cobbles consist of many resistant lithologies from the Rio Salado drainage to the west, particularly granite and metamorphic rocks from the Ladron Mountains, volcanic rocks from the volcanic plateaus of the transition zone, and limestone and sandstone from the Colorado Plateau. Stage II+ pedogenic calcium-carbonate horizons are near the surface due to the stripping of overlying Bt (? presumably) horizons. The terraces are eroded on both the east and west sides of the divide, and they are deeply eroded farther southeast by south-southeast headwater drainages descending to the next Rio Salado terrace (Qae of Machette, 1978a) to the south. The west sides of the terraces appear to be cut by younger faults that form a north-south graben (beyond the scope of this summary). The heights of the terraces above the Rio Grande suggest that they may grade to the top or just below the top of the maximum aggradation of ancestral Rio Grande deposits ~780 ka (Love et al., 2009), although Sion et al. (2020) correlated the high Rio Salado terraces to their Tio Bartolo surface (~70 m above the Rio Grande, ca. 610 ka).

Two units are shown as inset below the hanging-wall divide and must be younger than all the other units. In the big bowl (Division 3 south; Fig. 5), a paleo-arroyo several meters deep is filled with pebbly sand (unit 8 on Fig. 5). The filled arroyo cuts southwest across unit 4 and may cut the top of unit 3 farther out in the bowl. It is likely that the paleo-channel turned to the east and exited the bowl to the east similar to the modern channel, but at a higher level that is now completely eroded away.

At the south end of exposures on the divide between the southernmost erosional bowl and the incised, post-terrace channel to the southeast, the paleo-valley of the drainage is filled by unit 9, consisting of 4–5 m of thin gravels, pebbly sands, and thin brown clay beds. Although the exposures are in the erosional bowl north of the divide, the unit slopes to the south and pebble imbrications show transport to the south, indicating that the paleo-valley headwaters were farther north. Erosion of the south bowl of Division 6 has beheaded the drainage and reversed the direction of drainages into the bowl.

Dissection of the valley border of the Rio Grande has removed most of the footwall east of the Cliff fault and is increasingly removing the less-resistant sediments of the hanging wall. Unlike the flight of inset river terraces preserved on the east side of the Rio Grande (Love et al., 2009; Sion et al., 2020), only terraces related to the Rio Puerco and Rio Salado are documented on the west side of the valley.

ESTIMATE OF AMOUNT OF EROSIONAL STRIPPING OF THE TOP OF THE FOOTWALL AT THE SOUTHERN END OF FAULT TRACE DIVISION 4

One cannot assume that the present top of the footwall at BM "Cliff," at the southern end of fault trace Division 4, is the original top of the basin-fill deposits. If the 15 m of poorly sorted gravelly sand deposits of hanging-wall unit 5a above the highest, nearly horizontal reddish-brown clay and overlying soil are shed from the partially cemented footwall, it is possible to calculate the amount removed east of the fault. Although eolian sand from the west-southwest may have added to the sandy deposits, the sand may have been reworked uphill from distal sand deposits from the lower parts of the alluvial apron west of the scarp. Preliminary calculations of erosional stripping are shown in Figure 8. The hanging wall deposits are assumed to form a triangle with a horizontal base along 410 m to the west, a 2° slope of the alluvial surface of the hanging wall, and the 15 m of deposits at the fault. These measurements form an area of 3075 m^2, equivalent to cubic meters per meter of preserved hanging wall. The present slope of the eroded footwall is 7°, and the horizontal level of a conglomeratic unit at the top of the exposed fault is projected to the east where it crops out at the Rio Grande Valley margin, and the top of the footwall is 9.65 m above. The nearly equivalent triangle would be 224 m horizontal and 27.5 m vertical with an area of 3080 m^2. One could adjust the dimensions to make an exact match, but that precision would be more than the accuracy. Nonetheless, the calculation suggests that the 18 m of unit 1 may not be all of the strata of basin fill preserved on the less-offset south end of hanging-wall exposures.

CONCLUSIONS

This study has yielded the following results: First, although the normal, down-to-the-west Cliff fault trends almost due north overall, the fault deviates over short distances between N38°W to N28°E. The elevated footwall shows that the Cliff fault continues to the north-northeast, rather than veering to the northwest. Second, whereas previous studies showed that the Rio Puerco flowed to the southeast toward an ancestral Rio Grande, we determined that the Rio Salado flowed northeast toward the southeastward course of the Rio Puerco. At times, southeastward-directed gravel channels mixed clasts of both streams. Up-section, the channels appear to have Rio Salado clasts exclusively. The sediments delivered by these drainages to this part of the southern Albuquerque Basin probably pushed the Rio Grande to the east, against the western edge of the Joyita Hills. This dominant amount of sedimentation from these two drainages requires a revision of paleogeographic maps of the southern Albuquerque Basin (such as Lozinsky et al., 1991; Connell et al., 2013). Third, basin fill exposed on the footwall of the Cliff fault was deposited by two streams, other alluvial and perhaps playa sediments, and large eolian sand dunes. Compared to the proximal to distal basin fill of the Rio Puerco depositional system of the Albuquerque Basin documented farther north (e.g., Davis et al., 1993; Connell, 2008; Connell et al., 2013), the facies of basin fill along the Cliff fault has a wider variety of facies in the medial-to-distal positions of these deposits. Fourth, the exposed top of the footwall is not the depositional top of the basin fill here. Not only are formerly permeable beds of the footwall and the fault damage zone cemented with phreatic calcium carbonate up to the highest exposures, we calculate that as many as 27 m of the footwall have been eroded. Fifth, we delineated five generalized stratigraphic units of the hanging wall that record different phases of the fault's development through time. Upper parts of the footwall stratigraphic section may be preserved in the faulted and tilted southern end of the hanging-wall exposures (unit 1). Unit 2 consists of 25 m of mostly pebbly sand with a few minor, reddish-brown clay beds. The transport direction of many of the pebbly sand beds of the hanging wall continued to be to the south, southeast, or south-southwest and continued to be derived from the Rio Salado drainage and distributary alluvium that were bending southeastward near the alluvial fan–basin floor boundary west of the Cliff fault. The overlying 23 m of units 3 and 4, comprised of fine-grained beds, are dominated by wedge-shaped, reddish-brown playa clays interspersed with pebbly sands and pedogenic calcium carbonate horizons. Although some thick, reddish-brown, playa-like planar clay beds crop out on the footwall, the hanging wall reddish-brown clayey beds are thickest adjacent to the fault and wedge out to the west or southwest, away from the fault. These beds may record ponding due to offset along the fault, or damming by small, east-directed alluvial fans deposited toward the fault from a larger alluvial complex of the Rio Salado to the west. Beds within the units locally show some pebbly sand shed from the footwall. Unit 5 at the top of hanging-wall deposits is 13–15 m of poorly sorted, almost structureless pebbly sands, in contact with the fault in cyclic beds related to repeated normal movements along the fault, or in small channels flowing south, subparallel to the fault. These beds thin to the west and provide an estimate of the amount of erosion stripping the footwall as well as a possible constraint on the most recent events along the fault. Sixth, two elevated but extensively dissected terraces of the ancestral Rio Salado are deposited across the beveled hanging wall, fault, and footwall on the northern margin of the Rio Salado Valley and do not appear to be offset by the fault. These suggest that the fault has not ruptured the surface since early Middle Pleistocene time. Seventh, alluvial deposits within the southeast-directed valley (Division 7, unit 9) tributary to the Rio Salado Valley are deposited across the fault and are not offset by it, but they do record that the valley had headwaters farther north, in an area beheaded by the large, east-draining bowl near the south end of the fault (Division 6 south). Eighth, the largest erosional bowl in the hanging wall to the north (Division 3 south bowl, unit 8) contains deposits of a southwest-directed, arroyo-like paleo-valley that is cut into older units of the hanging wall and filled with reworked sediments from the footwall. Ninth, erosion of the western Rio Grande Valley margin has removed most evidence of episodes of terrace formation inset against the footwall, except in the Rio Salado and Rio Puerco Valleys. More detailed studies of the remarkably exposed hanging-wall strata will undoubtedly lead to a more detailed chronology of depositional and faulting episodes.

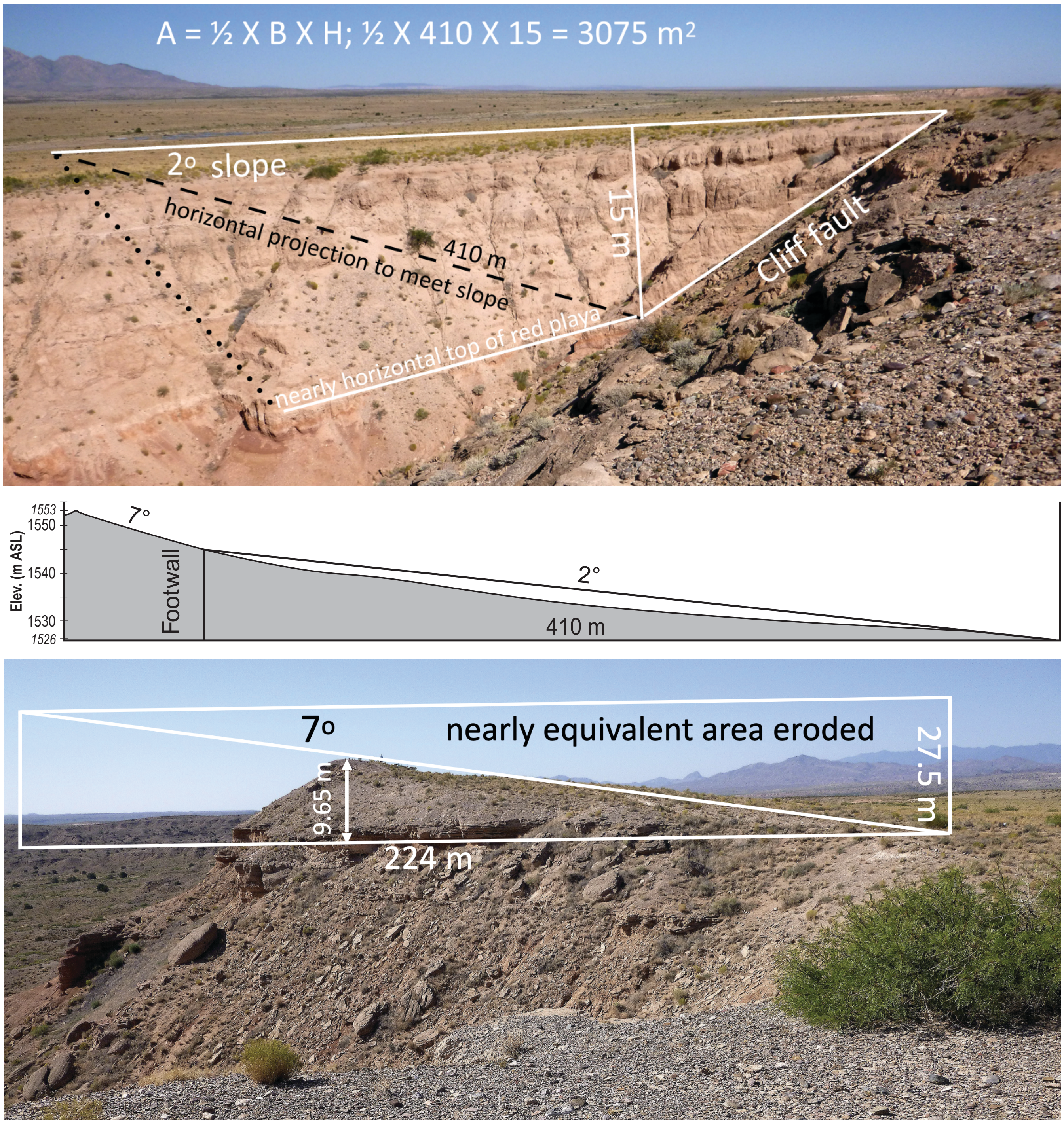

FIGURE 8. Estimates of the areas (or 1 m wide volumes) of sediments in the upper part of the hanging wall above the last playa bed and soil (unit 5a of Fig. 5) and the estimated height of the footwall removed by erosion to be deposited on the hanging wall. Area of triangle of hanging wall with 2° slope (A = ½ x B x H) = ½ x 410 m x 15 m = 3075 m^2, in comparison to the area of the triangle with 7° slope above the eroded footwall = ½ x 224 m x 27.5 m = 3080 m^2.

REFERENCES

Bryan, K., 1938, Geology and ground-water conditions of the Rio Grande depression in Colorado and New Mexico: Washington, D.C., Natural Resources Committee, Regional Planning, Part 6, Upper Rio Grande Basin, v. 1, pt. 2, sect. 1, p. 197–225.

Celep, E., 2017, Lithofacies analysis of the Sierra Ladrones Formation, southern Albuquerque basin N.M.: Implications for the Cliff fault activity during the early Pleistocene [M.S. thesis]: Socorro, New Mexico Institute of Mining and Technology, 94 p.

Connell, S.D., 2008, Refinements to the stratigraphic nomenclature of the Santa Fe Group, northwestern Albuquerque Basin, New Mexico: New Mexico Geology, v. 30, p. 14–35.

Connell, S.D., and McCraw, D.J., 2007, Preliminary Geologic map of the La Joya NW quadrangle, Socorro County, New Mexico: New Mexico Bureau of Geology and Mineral Resources, Open-file Geologic Map 140, scale 1:24,000, 8 p.

Connell, S.D., Love, D.W., Lucas, S.G., Koning, D.J., Derrick, N., Maynard, S.R., Morgan, G.S, Jackson-Paul, P.B., and Chamberlin, R., 2001, Stratigraphy and tectonic development of the Albuquerque Basin, central Rio Grande rift, *in* Field trip guidebook for the Geological Society of America, Rocky Mountain-South Central Section Meeting, Albuquerque, NM, Pre-meeting field trip: New Mexico Bureau of Mines and Mineral Resources, Open-file Report 0454A, p. 1–56.

Connell, S.D., Smith, G.A., Geissman, J.W., and McIntosh, W.C., 2013, Climatic controls on non-marine depositional sequences in the Albuquerque Basin, Rio Grande rift, north-central New Mexico, *in* Hudson, M.R., and Grauch, V.J.S., eds., New Perspectives on Rio Grande Rift Basins: From Tectonics to Groundwater: Geological Society of America, Special Paper 494, p. 383–425.

Davis, J.M., Lohmann, R.C., Phillips, F.M., Wilson, J.L., and Love, D.W., 1993, Architecture of the Sierra Ladrones Formation, central New Mexico: Depositional controls on the permeability correlation structure: Geological Society of America, Bulletin 105, p. 998–1007.

Denny, C.S., 1940, Tertiary geology of the San Acacia area, New Mexico: The Journal of Geology, v. 48, no. 1, p. 73–106.

Gile, L.H., Hawley, J.W., and Grossman, R.B., 1981, Soils and geomorphology in the Basin and Range area of southern New Mexico, *in* Guidebook to the Desert Project: New Mexico Bureau of Mines and Mineral Resources, Memoir 39, 222 p.

Gillespie, C.L., Grauch, V.J.S., Oshetski, K., and Keller, G.R., 2000, Principal facts for gravity data collected in the southern Albuquerque Basin and a regional compilation, central New Mexico: United States Geological Survey, Open file Report 00-490.

Grauch, V.J.S., and Connell, S.D., 2013, New perspectives on the geometry of the Albuquerque Basin, Rio Grande rift, New Mexico: Insights from geophysical models of rift-fill thickness: Geological Society of America, Special Paper 494, p. 427–462.

Hawley, J.W., ed., 1978, Guidebook to Rio Grande Rift in New Mexico and Colorado: New Mexico Bureau of Mines and Mineral Resources, Circular 163, 241 p.

Kelley, V.C., 1977, Geology of the Albuquerque Basin: New Mexico Bureau of Mines and Mineral Resources, Memoir 33, 60 p.

Lambert, P.W., 1968, Quaternary stratigraphy of the Albuquerque area, New Mexico [Ph.D. dissertation]: Albuquerque, University of New Mexico, 329 p.

Love, D.W., and Young, J.D., 1983, Progress report on the late Cenozoic geologic evolution of the lower Rio Puerco: New Mexico Geological Society, Guidebook 34, p. 277–284.

Love, D.W., McCraw, D.J., Chamberlin, R.M., Reiter, M., Connell, S.D., Cather, S.M., and Majkowski, M., 2009, Progress report on tracking Rio Grande terraces across the uplift of the Socorro magma body: New Mexico Geological Society, Guidebook 60, p. 415–424.

Lozinsky, R.P., Hawley, J.W., and Love, D.W., 1991, Geologic overview and Pliocene-Quaternary history of the Albuquerque Basin, central New Mexico, *in* Julian, B., and Zidek, J., eds., Field Guide to geologic excursions in New Mexico and adjacent areas of Texas and Colorado: New Mexico Bureau of Mines and Mineral Resources, Bulletin 137, p. 157–162.

Lueth, V.W., Chamberlin, R., Peters, L., and Love, D.W., 2016, An ^{49}Ar/^{39}Ar age and paleogeographic setting for the Riley Travertine, Socorro County, New Mexico: New Mexico Geological Society, Guidebook 67, p. 58–61.

Machette, M.N., 1978a, Geologic map of the San Acacia quadrangle, Socorro County, New Mexico: U.S. Geological Survey, Geologic Quadrangle Map GQ-1415, scale 1:24,000.

Machette, M.N., 1978b, Late Cenozoic geology of the San Acacia-Bernardo area, *in* Hawley, J.W., ed., Guidebook to the Rio Grande rift in New Mexico and Colorado: New Mexico Bureau of Mines and Mineral Resources, Circular 163, p. 135–137.

Machette, M.N., and McGimsey, R.G., 1983, Quaternary and Pliocene faults in the Socorro and western part of the Fort Sumner 1° x 2° quadrangle, New Mexico: U.S. Geological Survey, Miscellaneous Field Studies Map, v. MF-1465-A.

Machette, M.N., Long, T., Bachman, G.O., and Timbel, N.R., 1997, Laboratory data for calcic soils in central New Mexico: Background information for mapping Quaternary deposits in the Albuquerque Basin, laboratory data for calcic soils in central New Mexico: New Mexico Bureau of Mines and Mineral Resources, Circular 205, p. 1–63.

McCalpin, J.P., Olig, S.S., Harrison, J.B.J., and Berger, G.W., 2006, Quaternary faulting and soil formation on the County Dump fault, Albuquerque, New Mexico: New Mexico Bureau of Geology and Mineral Resources, Circular 212, 36 p.

McCraw, D.J., Love, D.W., and Connell, S.D., 2006, Preliminary geologic map of the Abeytas quadrangle, Socorro County, New Mexico: New Mexico Bureau of Geology and Mineral Resources, Open-file Report 121, scale 1:24,000.

Morgan, G.S., Lucas, S.G., and Love, D.W., 2009, Cenozoic vertebrate faunas from Socorro County, central New Mexico: New Mexico Geological Society, Guidebook 60, p. 321–336.

Olig, S.S., Eppes, M.C., Forman, S.L., Love, D.W., and Allen, B.D., 2011, Late Quaternary earthquakes on the Hubbell Spring fault system, New Mexico, USA: Evidence for noncharacteristic ruptures of intrabasin faults in the Rio Grande rift, *in* Audemard M., F.A., Michetti, A.M., and McCalpin, J.P., eds., Geological Criteria for Evaluating Seismicity Revisited: Forty Years of Paleoseismic Investigations and the Natural Record of Past Earthquakes: Geological Society of America, Special Paper 479, p. 47–77.

Personius, S.F., and Mahan, S.A., 2003, Paleoearthquakes and eolian-dominated fault sedimentation along the Hubbell Spring fault zone near Albuquerque, New Mexico: Bulletin of the Seismological Society of America, v. 93, p. 1355–1369.

Rinehart, A.J., Love, D.W., and Miller, P.L., 2014, Geologic map of the Black Butte 7.5-minute quadrangle, Socorro and Valencia Counties, New Mexico: New Mexico Bureau of Geology and Mineral Resources, Open-file Geologic Map 235, scale 1:24,000.

Sion, B.D., Axen, G.A., Phillips, F.M., and Harrison, J.B., 2016, Fluvial terraces in the lower Rio Salado valley: correlations, estimated ages, and implications for Quaternary faulting and for surface uplift above the Socorro magma body: New Mexico Geological Society, Guidebook 67, p. 235–247.

Sion, B.D., Phillips, F.M., Axen, G.J., Harrison, J.B.J., Love, D.W., and Zimmerer, M.J., 2020, Chronology of terraces in the Rio Grande rift, Socorro basin, New Mexico: Implications for terrace formation: Geosphere, v. 16, 22 p., https://doi.org/10.1130/GESo2220.1.

U.S. Geological Survey (USGS), n.d., Quaternary fault and fold database, Cliff fault No. 2111 (accessed 1/21/22).

Wright, H.E., 1946, Tertiary and Quaternary geology of the lower Rio Puerco area, New Mexico: Geological Society of America, Bulletin 57, p. 383–456.

Young, J.D., and Love, D.W., 2016, Grants obsidian in the Ceja Formation beneath the Llano de Albuquerque South of Belen: New Mexico Geological Society, Guidebook 67, p. 22–24.

Coyote skull in the badlands east of the Santa Fe Diner, San Marcial Basin. Photo by Lewis Gillard.